Communications on Applied Nonlinear Analysis
ISSN: 1074-133X
Vol 31 No. 8s (2024)

# Radiative Maxwell Nanofluid Flow over a Stretching Sheet Undergoing a Chemical Reaction

**Padmini[1], Jagadish V Tawade[2*], Pradeep Janthe[3]**

[1]VTU RC, Department of Mathematics, Bheemanna Khandre Institute of Technology, Bhalki, INDIA, [1]pskaji123@gmail.com

[2, 3]Vishwakarma University, Kondhwa(BK), Pune-411048, INDIA

[2]jagadish.tawade@vupune.ac.in, [3]pradeepjanthe@gmail.com

*Corresponding authors: Jagadish V. Tawade (jagadish.tawade@vupune.ac.in)

***Article History:***

***Received:*** *24-05-2024*

***Revised:*** *05-07-2024*

***Accepted:*** *23-07-2024*

**Abstract:**

Heat and mass transform properties of a 2-D electrically conducting incompressible Maxwell fluid over a stretching sheet were explored in presence of thermal radiation, heat generation/absorption, and chemical reactions. A numerical study of heat and mass transform processes occurring over stretching sheet is performed. Governing boundary layer equations for momentum, energy, & concentration are transformed into set of related ordinary differential equations using a stream function formulation. Then, using the BVP4C method, resultant nonlinear ordinary differential equations are numerically solved. Important research data are shown both graphically, including velocity, Lewis number (Le), Brownian motion parameter (Nb), concentration profiles, local skin friction coefficient, and rates of heat and mass transfer. Impacts of parameters across stretching surface, such as Maxwell parameter (k0), magnetic parameter (M), Biot number (Bi), elastic parameter (λ), Brownian motion parameter (Nt), and radiation parameter (Nr), are also investigated by numerical analysis in this study.

**Keywords**: Nano fluid,Maxwell, thermal radiation,stretching sheet, Biot number, Brownian motion parameter.

## 1. Introduction

In engineering and manufacturing sectors such as f crystal growth, fibber polymer sheet extrusion production, etc., it is important to investigate heat transfer in viscous fluid flows as well as heat transmission across sheets that are often expanding or contracting. The mechanized processes employed in the polymer industry to create high-quality sheets are also greatly influenced by the cooling rate. As a result, over the past few decades, numerous academics have invested a lot of time and energy into changing the kinematics flow in an effort to better manage the cooling rate. Various researchers have explored permeable stretching/shrinking sheet both with & without a slip regime at surface. The most significant study in this field, however, has been conducted by Sakiadis [1, 2, and 3], who carefully examined the boundary layer equations and underlying presumptions that control the flows on continuously expanding surfaces. The first calculation of MHD flow of a non-Newtonian fluid was done by Sarpakya [4]. use of Prandtl boundary layer theory prove to particularly beneficial in Newtonian fluids, as it allowed Navier-Stokes equations to be greatly reduced, making boundary layer equations simpler to manage. An elastic flat sheet that is stretched and has linear velocity

variations throughout its plane drives a two-dimensional Newtonian fluid flow from a fixed point; this is a situation that was first studied by Crane [5].

Grubka LG and Bobba KM [6] have investigated the heat transfer characteristics of a continuous stretched surface with variable temperature. Dutta BK and Gupta [7] studied as Stretching sheet cooling in different flow conditions. Jeng DR et. al. [8] the momentum and heat transmission in laminar boundary layer of a continuously moving surface with an arbitrary surface velocity and nonuniform surface temperature have been analyzed. AS Hydromagnetic, the nonsimilar solution corresponding to the viscous flow at a stagnation point on a wall moving at a constant velocity, was investigated by Chakrabarti A. Gupta [9]. Magneto-hydrodynamic flow of a power-law fluid across a stretched sheet was investigated by Andersson HI et al [10]. Afzal N [11] has studied Heat transfer from a stretching surface. Prasad KV et.al [12] studied Diffusion over a stretched sheet of chemically reactive species in a non-Newtonian fluid immersed in a porous media.

Nanofluids are defined as nanoparticles (less than 100 nm) suspended in basic fluids including oil, ethylene glycol, and water. A nanolayer to acts as a thermal suspension bridge between base fluid and solid nanoparticles facilitates heat transfer [13].
It can save energy in industrial settings by serving as a coolant. According to Ahmadreza [14], nanofluids are used as liquid cooling for computer processors, transformer cooling, electronic cooling solar water heating chillers, nuclear reactor coolant in grinding,domestic refrigerator chillers, engine cooling/vehicle thermal management, electronic cooling, defence, ships, and space technology, and power generation in nuclear reactors.

In applications such as heat burning in automobile engines, diesel electronic circuits drilling, lubrication, power exchangers, microelectronic fuel cells, pharmaceutical manufacturing, oil recovery, soil remediation, and detergency, nanofluids are used to transmit heat. Smaller heat exchangers used in automobiles and larger heat exchangers used in chemical processing plants both function more efficiently when nanofluids are present. Further research on heat radiation, chemical reaction, and nanoparticle presence in MHD flow of a maxwell fluid over a stretching sheet was conducted by G. K. Ramesh et al. [15]. Haritha et al.'s paper [16] focuses on mass and heat transfer of unsteady Maxwell fluid flow across a stretching surface under convective boundary conditions with naviger slip. Mahato et al. [17] looked at how a chemical reaction affected a nanofluid's magnetohydrodynamic motion and ability to transmit heat over a melting stretchy surface. Tawade et al. [18] created a unique MHD flow technique for UCM fluid over a permeable movable plate with internal heat effects. Thermal radiation has proven instrumental in creation of several higher energy conversion technologies that operate on high temperatures. Thermal radiation effects may be crucial in regulating heat transmission in the polymer manufacturing industry as certain heat-controlling factors affect the quality of the finished product. When the surface and its surroundings have significantly varying temperatures, thermal radiation's effects become more apparent. When the viscosity of the shear rate changed from low to high, Hassan et al.[19] examined the mass transfer and thermal energy of shear-thinning fluids using response surface techniques, Shafiq et.al.[20] examined effects of Walters_B nanoliquid flow across a radiative riga surface. The investigation sought to comprehend the effects of radiation, thermal slippage, and velocity on boundary layer flow in magnetohydrodynamics (MHD). In a study by

Dharmendar et al. [21], mass and heat transport mechanisms inside a Williamson nanofluid over porous media were examined.

Ramesh et.al [22] investigated the applied magneticfield and radiative heat transfer effects in the flow of Maxwell fluid past a stretching sheet. The MHD heat and mass transport of a Jeffrey fluid across a stretched sheet with chemical reaction and thermal radiation conducted by Narayana and Babu [23]. Slip effects on MHD boundary layer flow over an exponentially stretched sheet with suction/blowing and heat radiation was investigated by Mukhopadhyay [24]. The effect of radiation on boundary layer flow and heat transfer of a viscous fluid over an exponentially stretching sheet is studied by Sajid and Hayat [25]. Mandal and Pal [26] explored MHD boundary layer flow of micropolar nanofluid via a stretched sheet with non-uniform heat source/sink affected with thermal radiation. The impact of nonlinear thermal radiation on MHD boundary layer flow and melting heat transfer of micropolar fluid across a stretched surface with suspended fluid particles is investigated via a comprehensive numerical investigation by. Makinde et.al [27]. Thermal study of solar collector/storage system was investigated by Dhif, et.al. [28] applying a hybrid nanofluids method. Mebarek-Oudina[29] studied Numerical modelling of hydrodynamic stability in vertical annulus with heat source of different lengths. As Mebarek-Oudina[30] examined convective heat transfer between distinct base fluids' titania nanofluids in a cylindrical annulus with a separate heat source. Numerical study of magnetic hybrid nano-fluid natural convective flow in an adjustable porous trapezoidal enclosure was investigated by Chabani et al. [31]. Ree-Eyring liquid with changeable characteristics for hemodynamic flow was examined by Rajashekhar et.al [32]. They looked at the effects of mass and heat transfer on this peristaltic flow. Raza et.al. [33] studied the flow of magnetized convective Casson liquid via a porous channel with shrinking and stationary walls. Warke, et.al.[34] discussed the stagnation point flow of radiative magnetomicropolar liquid via a heated porous stretching sheet numerically in the presence of nonlinear heat generation/absorption. Mishra et.al [35] investigated MHD Williamson micropolar fluid flow on a non-linearly stretched sheet. Chemical reaction and Soret effect on an unsteady MHD heat and mass transfer fluid flow over an infinite vertical plate with radiation and heat absorption were investigated by Dharmendar and Shankar [36].

In addition, Anil Kumar and Dharmendar [37] investigated radiative Maxwell fluid flow over a stretching membrane that included nanoparticles and a chemical reaction using computer modelling. Borah et al. [38] investigated the effect of heat radiation and chemical reactions on the flow of thermally stratified boundary layers of Maxwell fluid over an expanding surface. To examine Maxwell fluids' MHD free convection flows across a porous plate, Kadja. et al. [39] used a unique method that relied on Caputo fractional model symmetry. Abbas et al. [40] studied the thermodynamic flow of a radiatively induced magneto-modified Maxwell fluid over a stretching sheet/cylinder.

In this current study, we explored the heat and mass transformation properties of a 2-D electrically conducting, incompressible Maxwell fluid as it flows over a stretching sheet. Our investigation considered various influencing factors, including thermal radiation, heat generation/absorption, and chemical reactions. We employed the BVP4C method to numerically solve the resulting set of nonlinear ordinary differential equations. The outcomes of our study are presented comprehensively, utilizing both graphical representations. These findings cover essential variables such as velocity,

Lewis number (Le), Brownian motion parameter (Nb), concentration profiles, local skin friction coefficient, as well as rates of heat and mass transfer.

## 2. Mathematical formulation:

Here in study, we consider non-Newtonian nanofluid flowing with the plane y=0 through a corresponding stretching surface, as demonstrated experimentally in Figure 1.

When the coordinate y is positive (y>0) and the stretching sheet is discovered to be perpendicular to it, the region where circulation is confined is shown. Moreover, we postulate that convection heats the stretching plate's bottom surface as hot fluid with temperature $T_w$, resulting in $h_f$ heat transfer coefficient. Moreover, we conjecture that convection heats bottom surface of stretching plate as a hot fluid with temperature $T_w$, resulting in a $h_f$heat transfer coefficient. Focus of this work is on a species-inclusive first-order homogeneous chemical reaction. Linear velocity of $u_w = ax$, where 'a' is the a +ve constant, stretches down x-axis.

A constant$B_0$ magnetic field is applied in a direction perpendicular to y-axis, which is direction of flow. Reynolds number of magnetic field was probably low. Therefore, compared to external magnetic field, induced magnetic field is much less.

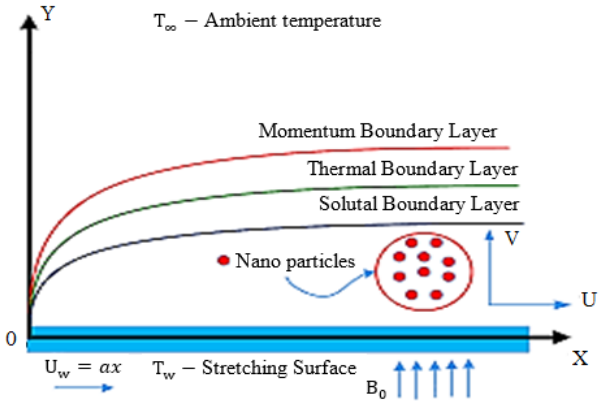


Figure 1. Physical configuration of model

The flow phenomena in dimensional form are as follows:

$$\frac{\partial u}{\partial x}+\frac{\partial \mathrm{v}}{\partial y}=0 \tag{1}$$

$$u\frac{\partial u}{\partial x}+\mathrm{v}\frac{\partial \mathrm{v}}{\partial y}+k_0\left(u^2\frac{\partial^2 u}{\partial x^2}+\mathrm{v}^2\frac{\partial^2 \mathrm{v}}{\partial y^2}+2u\mathrm{v}\frac{\partial^2 u}{\partial x\partial y}\right) = \mathrm{v}\frac{\partial^2 u}{\partial y^2}-\frac{\sigma {B_0}^2}{\rho_f}\left(u+k_0\mathrm{v}\frac{\partial u}{\partial y}\right)+\mathrm{g}\beta_{\mathrm{T}}(\mathrm{T}-\mathrm{T}_\infty)+\mathrm{g}\beta_{\mathrm{C}}(\mathrm{C}-\mathrm{C}_\infty)-\frac{\nu}{\mathrm{K}}\mathrm{u} \tag{2}$$

$$u\frac{\partial \mathrm{T}}{\partial \mathrm{x}}+\mathrm{v}\frac{\partial \mathrm{T}}{\partial y}=\alpha\frac{\partial^2 T}{\partial y^2}+\tau\left\{D_B\left(\frac{\partial C}{\partial y}\frac{\partial T}{\partial y}\right)+\frac{D_T}{T_\infty}\left(\frac{\partial T}{\partial y}\right)^2\right\}+\frac{Q_0}{\rho C_p}(\mathrm{T}-\mathrm{T}_\infty)-\frac{1}{\rho_f C_p}\frac{\partial q_r}{\partial y} \tag{3}$$

$$u\frac{\partial \mathrm{C}}{\partial \mathrm{x}}+\mathrm{v}\frac{\partial \mathrm{C}}{\partial y}=D_B\frac{\partial^2 C}{\partial y^2}+\frac{D_T}{T_\infty}\frac{\partial^2 T}{\partial y^2}-k_1(\mathrm{C}-\mathrm{C}_\infty) \tag{4}$$

Subject to boundary conditions

$$u = u_w(x) = ax, v = 0, -k\frac{\partial T}{\partial y} = h_f\left(T_f - T\right), C = C_w aty = 0$$

$$u = 0, T = T_\infty, asy \to \infty \tag{5}$$

$$\alpha = \frac{k}{(\rho C)_f}, \tau = \frac{(\rho C)_P}{(\rho C)_f}$$

Dimensionless heat generation/ absorption coefficient is ratio of the base fluid's heat capacity to that of nanoparticles.($C_\infty$) concentration in surrounding fluid differs from the static $C_\mathrm{w}$ concentration of nanoparticles at the surface. The estimated radioactive heat flow is calculated using the Rosseland approximation.

$$\boldsymbol{q_r} = -\frac{\mathbf{4}\boldsymbol{\sigma}^*}{\mathbf{3}\boldsymbol{K}^*}\frac{\partial T^4}{\partial y} \tag{6}$$

Since the variation in flow temperature is expected to be modest, we may obtain the linear function $T_4$by extending the equation in an Taylors series around T∞ and eliminating higher-order elements above first degree in (T - $T_\infty$).

We obtain

$$T^4 \approx 4{T_\infty}^3 T - 3{T_\infty}^4 \tag{7}$$

Then, Equation (3) becomes,

$$\frac{\partial q_r}{\partial y} = -\frac{16\boldsymbol{\sigma}^*{T_\infty}^3}{\mathbf{3}\boldsymbol{K}^*}\frac{\partial^2 T}{\partial y^2} \tag{8}$$

Introduce the following nondimensional variables:

$$\eta = \sqrt{\frac{a}{v}}y, \qquad \psi(x,y) = \sqrt{avx}f(\eta), \qquad \theta(\eta) = \frac{T - T_\infty}{T_f - T_\infty}, \qquad \varphi(\eta) = \frac{C - C_\infty}{C_f - C_\infty} \tag{9}$$

Defining $u = \frac{\partial \psi}{\partial y}$, and $v = -\frac{\partial \psi}{\partial x}$

When stream function ψ(x,y) is satisfied by equation (1), which is continuity.

Equation (9), when combined with Equations (2) and (4), yields following O.D Equation.

$$\mathrm{f}''' - \mathrm{M}^2\mathrm{f}' + (1 + \lambda\mathrm{M}^2)\mathrm{ff}'' - \mathrm{f}'^2 - \lambda(\mathrm{f}^2\mathrm{f}''' - 2\mathrm{ff}'\mathrm{f}'') + G_r\theta + G_m\varphi - K_1\mathrm{u} = 0 \tag{10}$$

$$(1 + \mathrm{Nr})\theta'' + \mathrm{Pr}\left(\mathrm{f}\theta' + \delta\theta + \mathrm{Nb}\varphi'\theta' + \mathrm{Nt}\theta''^2\right) = 0 \tag{11}$$

$$\varphi'' + \mathrm{LePrf}\varphi' + \frac{\mathrm{Nt}}{\mathrm{Nb}}\theta'' - \gamma\mathrm{LePr}\varphi = 0 \tag{12}$$

**Boundary conditions are:**

$$f(0) = 0, f'(0) = 1, \theta'(0) = -Bi\left(1 - \theta(0)\right), \varphi(0) = 1$$

$$f'(\infty) = 0, \theta(\infty) = 0, \varphi(\infty) = 0. \quad (13)$$

The prime represents differentiation with relation to η. f represents similarity function, $Pr = \frac{\nu}{\alpha}$ is Prandtl number, $Le = \frac{\alpha}{D_B}$ is Lewis number, $Bi = \frac{hf}{k}\sqrt{\frac{\upsilon}{\alpha}}$ is Biot number, $\lambda = ak_0$ is elastic parameter, $\delta = Q_0/(\rho C_P a)$ is heat generation/absorption parameter, $M = B_0\sqrt{\frac{\sigma}{(\rho_f a)}}$is magnetic parameter, $Nb = \frac{((\rho C)_P D_B(C_w - C_\infty))}{(\rho C)_f \upsilon}$ is Brownian motion parameter and , $Nt = \frac{((\rho C)_P D_T(T_w - T_\infty))}{(\rho C)_f T_\infty}$is thermophoresis parameter, $Nr = \frac{16\boldsymbol{\sigma}^* {T_\infty}^3}{\boldsymbol{3K}^*}$ is radiation parameter, $Gr = \frac{\upsilon g \beta_T (T_w - T_\infty)}{(u_0)^3}$ Grashaff number, $Gm = \frac{\upsilon g \beta_C (C_w - C_\infty)}{(u_0)^3}$ Grashaff number, $k_1 = \frac{\upsilon k(C_w - C_\infty)}{(u_0)^2}$is thePorous parameter.
It is believed that local Sherwood number $Sh_x$, local Nusselt number $N_{ux}$, and skin friction coefficient $C_f$are

$$C_f = \frac{\tau_w}{\rho u_w^2}, Nu_x = \frac{x q_w}{k(T_w - T_\infty)}, \qquad Sh_x = \frac{x h_x}{D_B(C_w - C_\infty)} \quad (14)$$

Where mass flow and surface heat are represented by $h_m$ and $q_w$, respectively, and shear stress is denoted by $\tau_w$:

$$\tau_w = \mu(1+\lambda)\left(\frac{\partial u}{\partial y}\right)_{y=0}, \qquad q_w = -k\left(\frac{\partial T}{\partial y}\right)_{y=0}, h_m = -D_B\left(\frac{\partial C}{\partial y}\right)_{y=0} \quad (15)$$

The similarity transformation provides the following changes to non-dimensional representations of Nusselt number,Skin friction and Sherwood number:

$$.{Re_x}^{1/2} C_f = (1+\lambda) f''(0), \ \frac{Nu_x}{{Re_x}^{1/2}} = -\theta'(0), \quad \frac{Sh_x}{{Re_x}^{\frac{1}{2}}} = -\varphi'(0) \quad (16)$$

Where $Re_x = \frac{x u_w}{\upsilon}$is local Reynolds number

## 3. Numerical Solution

Using provided boundary conditions (13), the bvp4c MATLAB solver is used to be find numerical solutions to equations (10)– (12). Given set of ordinary differential equations, we can solve them using this numerical approach. First order differential equations (17)– (26) are created from the system of equations (10)–(13) in order to do the bvp4c coding, as shown in the appendix below.

$$f = y(1) \quad (17)$$

$$f' = y(2) \quad (18)$$

$$f'' = y(3) \quad (19)$$

$$\theta = y(4) \quad (20)$$

$$\theta'' = y(5) \quad (21)$$

$$\varphi = y(6) \quad (22)$$

$$\varphi' = y(7) \qquad (23)$$

$$f''' = \text{yy1} = \left(\frac{1}{(1-\lambda*y(1)*y(1))}\right) * (M*M*y(2) - (1+\lambda*M*M)*y(1)*y(3) + y(2)*y(2) - 2*\lambda*y(1)*y(2)*y(3) - Gr*y(4) - Gm*y(6)) \qquad (24)$$

$$\theta'' = \text{yy2} = \frac{-1}{(1+Nr)} * Pr * (y(1)*y(5) + \delta*y(4) + Nb*y(7)*y(5) + Nt*y(5)*y(5)) \qquad (25)$$

$$\varphi'' = \text{yy3} = (-\text{Le}*\text{Pr}*\text{y}(1)*\text{y}(7) - (\text{Nt}/\text{Nb})*\text{yy2} + \gamma*\text{Le}*\text{Pr}*\text{y}(6)) \qquad (26)$$

With boundary conditions

For$\eta = 0;\ y(1) = 0, y(2) = 1, y(5) = -Bi\big(1 - y(4)\big), y(6) = 1.$

for$\eta = \infty; y(2) = 0, y(4) = 0, y(6) = 0.$ (27)

Seven initial conditions are needed to obtain the answer because there are seven ODEs. However, the only initial condition in equation (27) is five. Thus, for y(3) and y(7), reasonable initial predictions are expected. Moreover,

At$\eta_\infty = 2$, a finite point at infinity, we impose the boundary condition. I.e., the domain of the issue is restricted to [0, 2]. The computed solution will converge if the error in values of y (2), y (4), and y(6) is less than $10^{-2}$. If the error tolerance is exceeded, the procedure is repeated until the solution condition is satisfied. At first, many presumptions are made.

## 4. Results and discussion:

The results of our study, along with their discussion, are presented through various graphs, each depicting different aspects of the behavior of the 2-D electrically conducting Maxwell fluid over the stretching sheet. The set of graphs may focus on sensitivity analysis, showing how the chosen parameters such as Maxwell parameter ($k_0$), magnetic parameter (M), Biot number (Bi), elastic parameter (λ), Brownian motion parameter (Nt), and radiation parameter (Nr) impact the flow and transport properties. Sensitivity analysis helps in identifying the most influential parameters and their effects on the system behavior.

Each graph would be accompanied by a detailed discussion, interpreting the observed trends, comparing different scenarios, and providing insights into the underlying physics of the problem. Overall, the graphical representation of results facilitates a comprehensive understanding of the studied phenomena and aids in drawing meaningful conclusions.

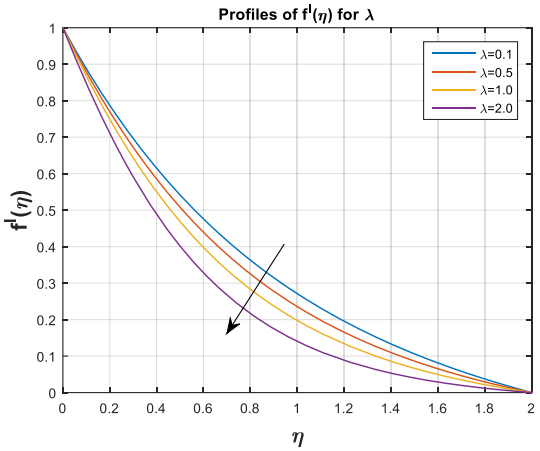


**Figure 2:** As elastic parameter λ increases, boundary layer thickness and velocity distribution both decrease.

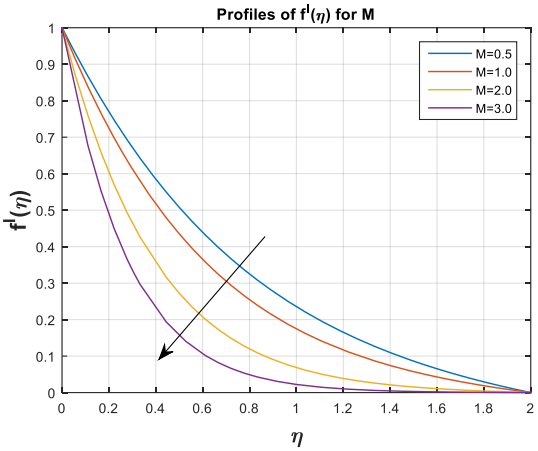


**Figure 3:** Illustrates the change in velocity profile for various Magnetic parameter (M) values. Velocity profile in boundary region reduces as the magnetic parameter values rise.

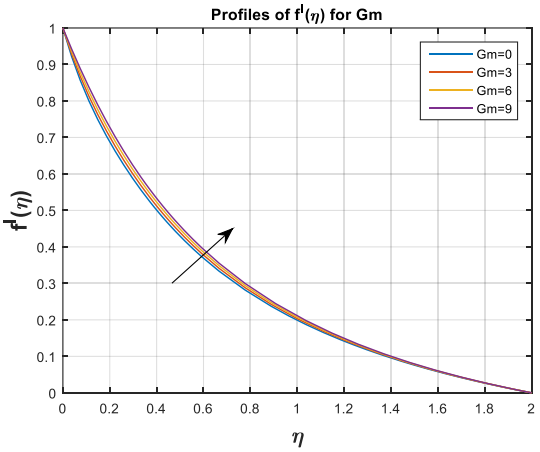


**Figure 4:** velocity profile modifications for different mass Grashof number (Gm) values are shown. The figure illustrates how the velocity parameter increases for different mass Grashof number (Gm) values.

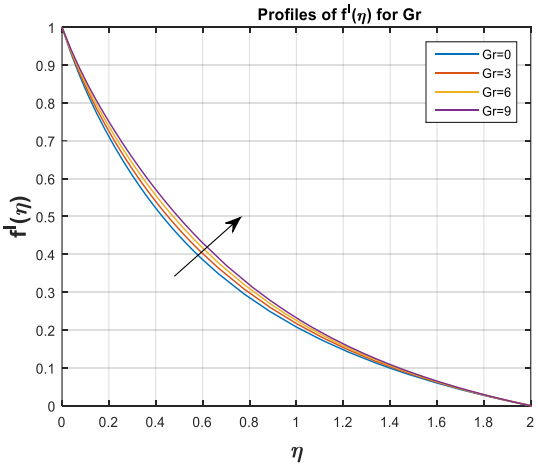


**Figure 5:** Velocity profile modifications for different values of Grashof number (Gr) are shown. Aforementioned plot demonstrates the velocity parameter increases as Grashof number (Gr) grows.

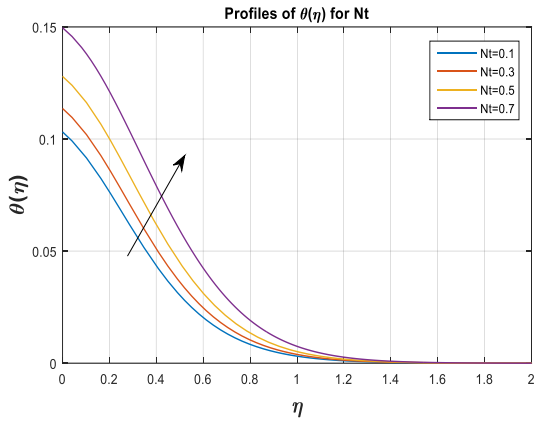


**Figure 6:** Temperature flow in boundary layer of thermal energy is seen when thermophoresis parameter Nt is adjusted. Thermophoresis is a force of transport triggered by a temperature differential. A force of transport called thermophoresis is brought about by a temperature difference. Temperature raises result from higher surface temperatures brought on by thicker boundary layers as a result of higher Nt.

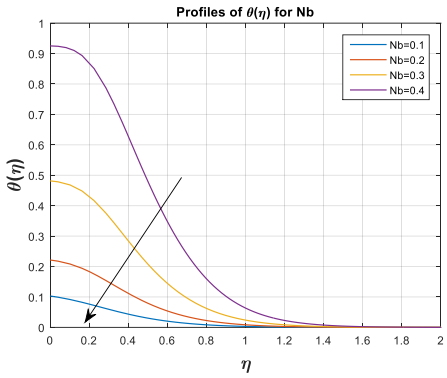


**Figure 7**: Temperature distribution of thermal boundary layer is shown for various Brownian motion Nb values. Brownian motion provides an explanation for temperature flux in thermal boundary layer. This uneven mobility speeds up the collisions between the fluid's molecules and nanoparticles. As Nb increases, representing stronger Brownian motion effects, the temperature distribution may exhibit distinct characteristics.

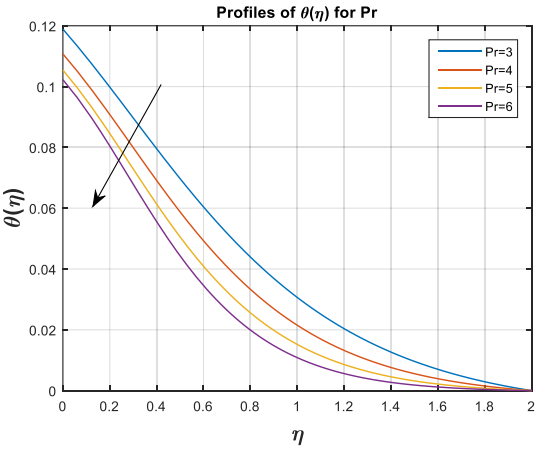


**Figure 8:** shows effect parameter on temperature of Prandtl number. Reduced thermal conductivity results in a higher Pr value, which in turn lowers thermal boundary layer's thickness andrate at which heat is transmitted over boundary surface. As a consequence of these physical processes, the temperature profile significantly drops.

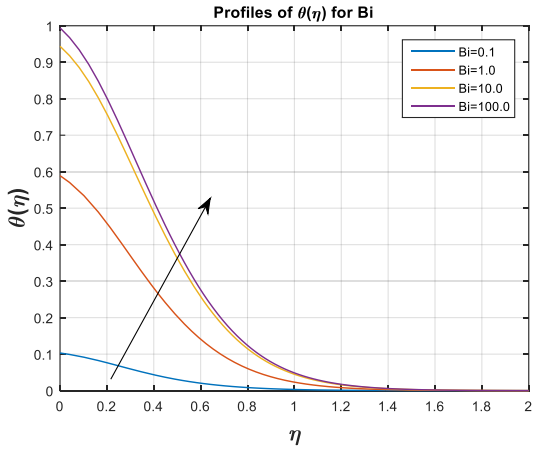


**Figure 9:** As the number of Biots grows, it has been observed that the temperature in the area near the boundary rises quickly. Because of convective high temperature transmission at plate's surface, thermal boundary layer thickens, causing this to happen.

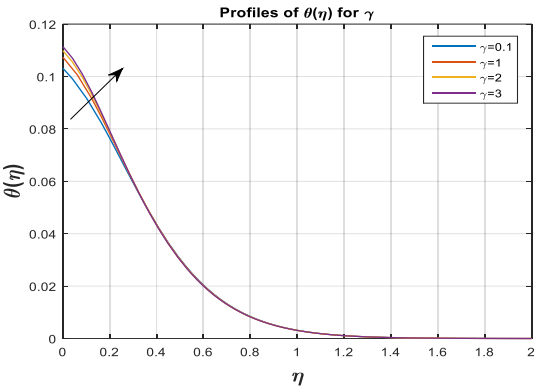


**Figure 10(a)**

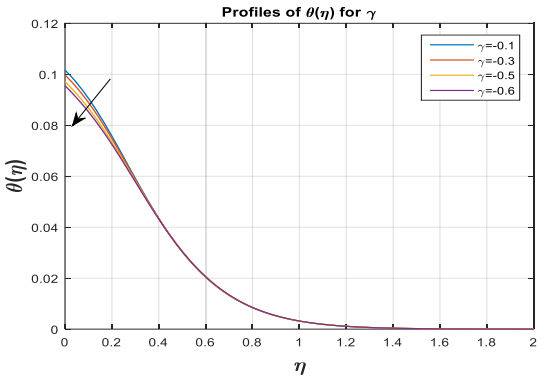


**Figure 10(b)**

**Figures 10(a) and 10(b)**: For both the positive and negative situations, Figures 5a and 5b show the temperature distribution for different values of chemical reaction parameters. On one hand, thermal boundary layer is strengthened when the damaging chemical reaction ($\gamma > 0$) in boundary layer is transformed into thermal energy or heat; on other hand, temperature of fluid drops when the generating chemical reaction ($\gamma < 0$) is present..

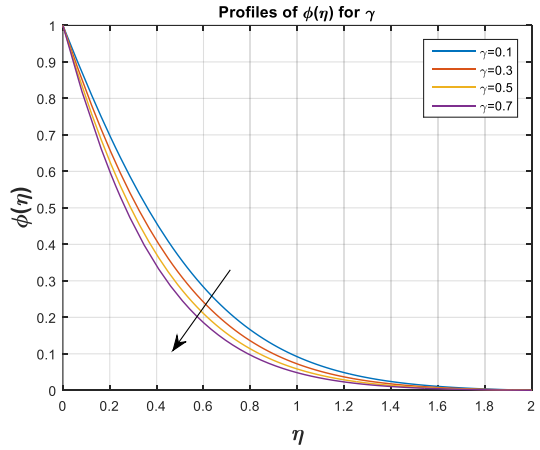


**Figure 11**:Araise in a chemical reaction parameter results in a thinner concentration boundary layer, while a reduction in chemical molecular diffusivity causes a little dip in the concentration profile.

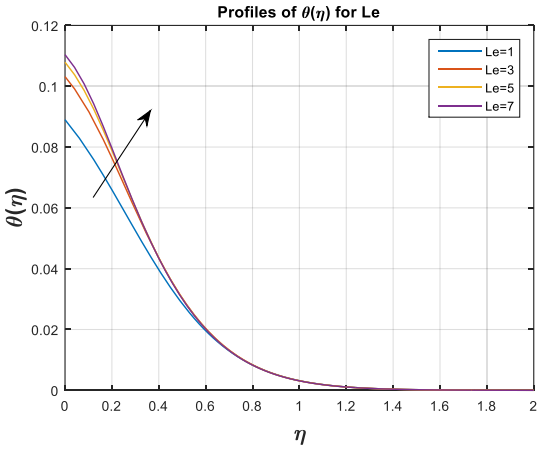


**Figure 12**: Lewis phone number Le is a symbol for the link between mass and heat. When mass and heat are being transferred concurrently, this criteria is employed to measure fluid flow. It is possible to compare the thermal layer thicknesses using the Lewis number. The Brownian diffusion coefficient and thermal diffusivity are both enhanced when the Lewis number rises. The result is a rise in temperature.

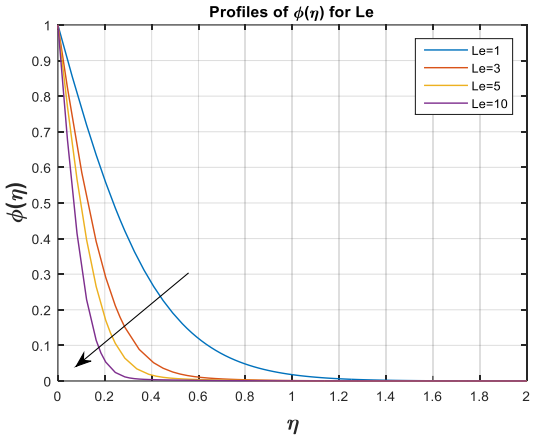


**Figure 13**: The Lewis number of mass diffusivity versus heat correlation coefficient is denoted as Le. The term "fluid flow" describes the simultaneous transport of mass and heat. Since, Lewis number may be used to compare the thickness of hot and cold border layers. Lewis goes up in rank. This data points to a hypothesis that concentration drops with increasing temperature.

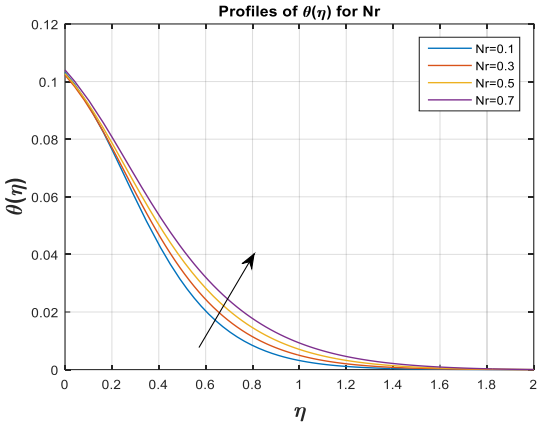


**Figure 14.** The temperature curve is shown for a range of radiation parameter Nr values. Since they greatly improve surface heat transfer and hence make fluid much hotter, increases in Nr figures have been demonstrated to improve temperature distribution**.**

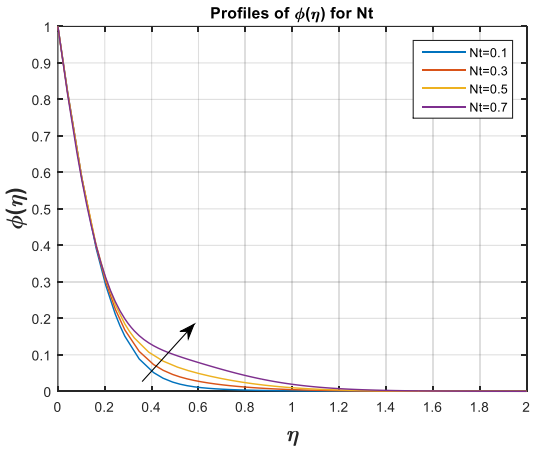


**Figure 15:** Displays the concentration distribution in thermal boundary layer for numerous values for thermophoresis parameter Nt. Thickness of concentration boundary layer and enhancement of thermophoresis strength both lead to better concentration**..**

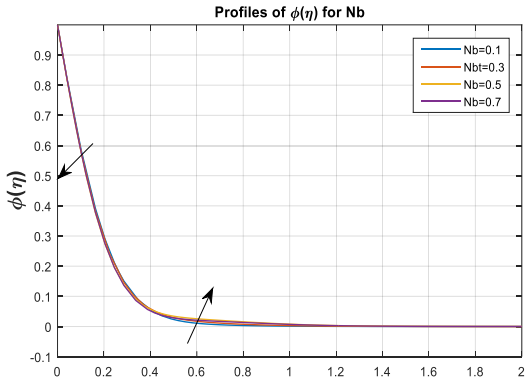


**Figure 16:** As the surface concentration of Nb grows, fluid's concentration decreases. When boundary layer warms due to Brownian motion, particles move out of the fluid regime. However, when one gets closer to the surface, the inverse trend becomes apparent.

## 5. Conclusion:

A two-dimensional Maxwell fluid that is incompressible and stable was studied in relation to chemical interactions with nanoparticles and thermal radiation. fluid was considered to be transporting mass and heat across a stretching sheet. Through quantitative analysis, we identified and evaluated the

impact of several embedded thermophysical parameters on the velocities, concentrations, and temperatures. The important findings are as below.

1. For an increase in the elastic parameter, both the boundary layer thickness and velocity distribution decrease.
2. The velocity parameter increases for different values of the mass Grashof number (Gm).
3. The velocity parameter increases as the Grashof number (Gr) grows.
4. Higher surface temperatures, resulting from thicker boundary layers due to a higher thermophoresis parameter (Nr), lead to temperature increases.
5. As Brownian motion (Nb) increases, representing stronger Brownian motion effects, the temperature distribution may exhibit distinct characteristics.
6. As the number of Biots increases, it has been observed that the temperature near the boundary area rises quickly.

**Author contribution statement:**

The authors confirm their contribution to the paper as follows:

**Study conception and design**: Padmini, Jagadish V Tawade;

**Data collection:** Pradeep G.Janthe, Padmini,

**Analysis and interpretation of results:** Padmini, Jagadish V Tawade, Pradeep G.Janthe;

**Draft manuscript preparation:** Padmini, Jagadish V Tawade, Pradeep G.Janthe;

All authors reviewed the results and approved the final version of the manuscript.

**Composing a data availability statement:**

- what the nature of the data: No separate data required for this specified work.
- where the data can be accessed: Not Applicable
- why there are any restrictions on data access: Not Applicable

**Competing interests:** The authors have declared that no competing interests exist.

**Declaration:** The authors declare that they have no known competing financial interests or personal relationships that could have appeared to influence the work reported in this paper.

**References**

[1] B. C Sakiadis, Boundary-layer behavior on continuous solid surfaces: I. boundary-layer equations for two-dimensional and axisymmetric flow, AIChE Journal 7 (1) (1961) 26–28.
[2] B.C Sakiadis, Boundary-layer behavior on continuous solid surfaces II. the boundary layer on a continuous flat surface, AIChE Journal 7 (2) (1961) 221–225.
[3] B. C. Sakiadis, Boundary-layer behavior on continuous solid surfaces III. the boundary layer on a continuous cylindrical surface, AIChE J 7 (3) (1961) :467–472
[4] Sarpakaya T Flow of non-Newtonian fluids in a magnetic field. AIChE J(7) (1961):324–328
[5] Crane Flow past a stretching plate. Z Angew Math Phys 21(1970):645–647
[6] Grubka LG, BobbaKM Heat transfer characteristics of a continuous stretching surface with variable temperature. *J. Heat Transfer*. (Feb 1985), 107(1): 248-250
[7] Dutta BK, Gupta AS Cooling of a stretching sheet in a various flow. Ind. Eng. Chem. Res. (1987), 26, 2, 333–336

[8] Jeng DR, Chang TCA, Dewitt KJ Momentum and heat transfer on a continuous surface. J Heat Transf 108:532–539
[9] Chakrabarti A, Gupta AS Hydromagnetic flow and heat transfer over a stretching sheet. Q Appl Math (1979) 37:73–78
[10] Andersson HI, Bech KH, Dandapat BS Magneto- hydrodynamic flow of a power-law fluid over a stretching sheet. Int J Non-Linear Mech27 (1992):929–936
[11] Afzal N Heat transfer from a stretching surface. Int J Heat Mass Transfer (1993) 36:1128–1131
[12] Prasad KV, AbelS, Datti PS Diffusion of chemically reactive species of a non-Newtonian fluid immersed in a porous medium over a stretching sheet. Int J Non-Linear Mech (2003)38:651–657.
[13] Choi SUS "Enhancing thermal conductivity of fluids with nanoparticles,International Mechanical Engineering Congress and Exposition", San Francisco, USA, ASME, FED 231/MD, vol66, (1995), pp.99–105.
[14] Ahmadreza, A. B. "Application of nanofluid for heat transfer enhancement",(2013), PID: 2739168, EEE-5425.
[15] G. K. Ramesh, B. J. Gireesha, T. Hayat and A. Alsaedi MHD Flow of Maxwell Fluid Over a Stretching Sheet in the Presence of Nanoparticles, Thermal Radiation and Chemical Reaction: A Numerical StudyJournal of Nanofluids (2015) Vol. 4, pp. 1–7,
[16] Haritha, Y.Devasena and B.Vishali MHD Heat and Mass Transfer of the Unsteady Flow of a Maxwell Fluid over a Stretching Surface with Navier Slip and Convective Boundary Conditions Global Journal of Pure and Applied Mathematics. ISSN 0973-1768 Volume 13, Number 6 (2017), pp. 2169-2179
[17] G. K. Mahato, B. K. Mahatha, R. Nandkeolyar, and B. Patra The effects of chemical reaction on magnetohydrodynamic flow and heat transfer of a nanofluid past a stretchable surface with melting AIP Conference Proceedings (2020)2253(1):020011
[18] J.V TAwade, Mahadev Malikarjun Biradar; Shaila Sangangouda Benal A new approach of MHD flows for UCM fluid over a permeable moving plate with space and temperature dependent internal heat generation/absorption *AIP Conference Proceedings* (2020)2236, 060002
[19] M. Hassan, F. Mebarek-Oudina, A. Faisal, A. Ghafar, A.I. Ismail, Thermal energy and mass transport of shear thinning fluid under effects of low to high shear rate viscosity, Int. J. Thermofluids 15 (2022), 100176.
[20] A. Shafiq, F. Mebarek-Oudina, T.N. Sindhu, G. Rassoul, Sensitivity analysis for Walters' B nanoliquid flow over a radiative Riga surface by RSM, Sci. Iran. 29 (3) (2022) 1236–1249,.
[21] Y. Dharmendar Reddy, F. Mebarek-Oudina, B.S. Goud, A.I. Ismail, Radiation, velocity and thermal slips effect toward MHD boundary layer flow through heat and mass transport of Williamson nanofluid with porous medium, Arabian J. Sci. Eng. 47 (12) (2022) 16355–16369,
[22] G. Ramesh, B. Gireesha, T. Hayat, A. Alsaedi, MHD flow of Maxwell fluid over a stretching sheet in the presence of nanoparticles, thermal radiation and chemical reaction: a numerical study, J. Nanofluids 4 (1) (2015) 100–106.
[23] P.S. Narayana, D.H. Babu, Numerical study of MHD heat and mass transfer of a Jeffrey fluid over a stretching sheet with chemical reaction and thermal radiation, J. Taiwan Inst. Chem. Eng. 59 (2016) 18–25.
[24] S. Mukhopadhyay, Slip effects on MHD boundary layer flow over an exponentially stretching sheet with suction/blowing and thermal radiation, Ain Shams Eng. J. 4 (3) (2013) 485–491.
[25] M. Sajid, T. Hayat, Influence of thermal radiation on the boundary layer flow due to an exponentially stretching sheet, Int. Commun. Heat Mass Tran. 35 (3) (2008) 347–356.
[26] D. Pal, G. Mandal, Thermal radiation and MHD effects on boundary layer flow of micropolar nanofluid past a stretching sheet with non-uniform heat source/sink, Int. J. Mech. Sci. 126 (2017) 308–318.
[27] O.D. Makinde, K.G. Kumar, S. Manjunatha, B.J. Gireesha, Effect of nonlinear thermal radiation on MHD boundary layer flow and melting heat transfer of micro-polar fluid over a stretching surface with fluid particles suspension, in: Defect and Diffusion Forum, vol. 378, Trans Tech Publ, (2017), pp. 125–136
[28] K. Dhif, F. Mebarek-Oudina, S. Chouf, H. Vaidya, Ali J. Chamkha, Thermal analysis of the solar collector cum storage system using a hybrid-nanofluids, J. Nanofluids 10 (4) (2021) 634–644,
[29] F. Mebarek-Oudina, Numerical modeling of the hydrodynamic stability in vertical annulus with heat source of different lengths, Eng. Sci. Technol. 20 (4) (2017) 1324–1333
[30] F. Mebarek-Oudina, Convective heat transfer of titania nanofluids of different base fluids in cylindrical annulus with discrete heat source, Heat Tran. Asian Res. 48 (2019) 135–147

[31] I. Chabani, F. Mebarek-Oudina, H. Vaidya, A.I. Ismail, Numerical analysis of magnetic hybrid Nano-fluid natural convective flow in an adjusted porous trapezoidal enclosure, J. Magn. Magn Mater. 564 (2) (2022), 170142.

[32] C. Rajashekhar, F. Mebarek-Oudina, H. Vaidya, K.V. Prasad, G. Manjunatha, H. Balachandra, Mass and heat transport impact on the peristaltic flow of Ree- Eyring liquid with variable properties for hemodynamic flow, Heat Transfer 50 (5) (2021) 5106–5122

[33] J. Raza, F. Mebarek-Oudina, L. Ali Lund, The flow of magnetised convective Casson liquid via a porous channel with shrinking and stationary walls, Pramana - J. Phys. 96 (2022) 229

[34] A.S. Warke, K. Ramesh, F. Mebarek-Oudina, A. Abidi, Numerical investigation of the stagnation point flow of radiative magnetomicropolar liquid past a heated porous stretching sheet, J. Therm. Anal. Calorim. 147 (12) (2022) 6901–6912

[35] Pankaj Mishra, Dhirendra Kumar, Y. Dharmendar Reddy, B. Shankar Goud, MHD Williamson micropolar fluid flow pasting a non-linearly stretching sheet under the presence of non linear heat generation/absorption, J. Indian Chem. Soc. 100 (Issue 1) (January 2023), 100845.

[36] Y. Dharmendar Reddy, B. Shankar Goud, Chemical reaction and Soret effect on an unsteady MHD heat and mass transfer fluid flow along an infinite vertical plate with radiation and heat absorption, J. Indian Chem. Soc. 99 (Issue 11) (November 2022), 100762.

[37] M. Anil Kumar, Y. Dharmendar Reddy Computational modelling of radiative Maxwell fluid flow over a stretching sheet containing nanoparticles with chemical reaction. Journal of the Indian Chemical Society 100 (2023) 100877

[38] Rupjyoti Borah , Ashimjyoti Boruah , DebasishDey and MadhuryaHazarikaIV Thermally Stratified Boundary Layer Flow Of Maxwell Fluid Over An Elongating Surface With The Results Of Thermal Radiation High Technology Letters (2023)29(7):124-133

[39] Aslam K, Zafar AA, Shah NA, Almutairi B. MHD Free Convection Flows for Maxwell Fluids over a Porous Plate via Novel Approach of Caputo Fractional Model. *Symmetry*. (2023)15(9):1731 2023, 15, 1731.

[40] Abbas N, Shatanawi W, Hasan F, Mustafa Z. Thermodynamic flow of radiative induced magneto modified Maxwell Sutterby fluid model at stretching sheet/cylinder. Sci Rep. (2023) Sep 25; 13(1):16002.